The comparative analysis of energy dissipation behaviour of woven and UD para-aramid fabrics

DOI: 10.35530/IT.075.05.202470

ALİ ARI MEHMET KARAHAN

ABSTRACT – REZUMAT

The comparative analysis of energy dissipation behaviour of woven and UD para-aramid fabrics

This research examines how impact energy spreads across para-aramid fabrics, comparing woven and unidirectional types, using 2-D Thin Plate Spline analysis. The experiment involved dropping a weighted hemisphere onto fabric samples and measuring their deformation across different layer counts. To assess how yarn orientation affects energy dispersion, panels with 0º/90º and 0º/90º/±45º configurations were tested. By analysing the fabric's shape changes under impact, the study revealed patterns of energy propagation. Calculations of bending energy and expansion factors provided insights into this behaviour. The findings indicate that unidirectional fabrics outperform woven structures in distributing impact energy across their surface. Moreover, incorporating ±45º fibre reinforcements in both fabric types enhances energy dispersion and mitigates impact effects.

Keywords: *Thin Plate Spline (TPS) method, impact energy, woven and unidirectional para-aramid fabric*

Analiza comparativă a comportamentului de disipare al energiei a materialelor para-aramidice ţesute și unidirecționale

Acest studiu examinează modul în care energia de impact se răspândește în țesăturile para-aramidice, comparând tipurile țesute și unidirecționale, utilizând analiza 2-D Thin Plate Spline. Experimentul a implicat contactul dintre o emisferă cu greutate ridicată și eșantioanele de țesături și determinarea deformării acestora în diferite straturi. Pentru a evalua modul în care orientarea firului afectează dispersia energiei, au fost testate panouri cu configurații 0º/90º și 0º/90º/±45º. Analizând modificările formei țesăturii sub impact, studiul a relevat modele de propagare ale energiei. Calculele energiei solicitării la încovoiere și ale factorilor de expansiune au oferit informații despre acest comportament. Rezultatele indică faptul că țesăturile unidirecționale depășesc structurile țesute în distribuirea energiei de impact pe suprafața lor. În plus, încorporarea de armături cu fibre la ±45º în ambele tipuri de țesături îmbunătățește dispersia energiei și atenuează efectele de impact.

Cuvinte-cheie*: metoda Thin Plate Spline (TPS), energie de impact, material para-aramidic ţesut și unidirecțional*

INTRODUCTION

Utilizing ballistic shielding effectively prevents projectiles from penetrating during collisions. Furthermore, it must disperse the kinetic energy that is transferred through the armour. Undoubtedly, this kinetic energy is accountable for the dynamic deformations that have the capability to specifically impact the physique of the individual wearing the armour. The impact caused by the movement of the protective armour is referred to as “Behind Armour Blunt Trauma” (BABT). Even if the impact does not penetrate, it has the potential to cause significant localized damage to an area. Multiple research investigations were conducted to assess the magnitude of deformations resulting from ballistic protection [1].

Ballistic gelatin [2, 3] and plastilina [4] are commonly employed as witness materials to assess the performance of armours in terms of BABT measurement. The latter is user-friendly, reusable, cost-effective, and maintains its distorted configuration after impact [4]. Before conducting ballistic testing, it is necessary to calibrate the texture of these materials by specified criteria outlined in the standards. The primary standards include STANAG 2920, AEP 2920, NIJ, HOSDB, and VPAM. NIJ measures the indentation depth of Roma® #1 plastilina, while VPAM measures the volume of the depression in plastilina red Weible® after ballistic impacts. The “drop test” is the most traditional calibration test for plastilina, and its process is outlined in the NIJ standard [5].

Although the drop test approach is straightforward for users in ballistic laboratories, it has been the focus of extensive research, particularly on plastilina Roma®#1. For instance, Roberts et al. [6] conducted drop tests using a standardized protocol, but they varied the initial height of the steel ball. The authors conducted an experimental assessment of the impact of this parameter on the ultimate depth of penetration in drop experiments. Based on their findings, they additionally built a framework to describe the mechanical behaviour of plastilina. Mates et al. [7] conducted a study where they used 3D image

correlation to quantify the changes in velocity and penetration depth of a steel ball over time during drop testing. Hernandez et al. [8] conducted a series of drop tests using steel balls of varied diameters, which were dropped from varying heights. The scientists examined the response of the plastilina in terms of penetration depth during a relatively short period, compared to two previous investigations. Finally, Gilson et al. [9] conducted a comparative analysis between the previously stated research and performed drop tests on samples of plastilina red Weible®. The researchers noted that the composition of the plastilina and the measuring technique employed during the drop test can impact the interpretation of the plastilina's calibration of its texture.

Numerous studies have explored the behaviour model of textile fibres and fabrics in response to ballistic impact, attempting to identify and forecast this behaviour through the development of models [10–14]. However exact estimation of this behaviour and ballistic performance of fabric from the fibre qualities has not been possible especially when the bullet size is small because bullet-fabric interaction is a very instantaneous and complex event [15].

In biology and other disciplines, one is frequently interested in describing the difference in shape (or size and shape) between two or more objects. A measure of shape distance, such as the full Procrustes distance, gives us a numerical measure of shape comparison, but this global shape measure does not indicate locally where the objects differ and the manner of the difference. The biological goal in many studies is to depict or describe the morphological changes in a study.

The morphometric techniques we used here were shape analysis landmark coordinates and image averaging thin-plate spline (TPS) [16]. Bookstein [17] developed thin-plate spline analysis as a morphometric approach for comparing landmark configurations in two or more specimens.

The concept of thin-plate spline was first applied to the analysis of plane shapes by Bookstein [18]. In such approaches, a thin-plate is understood as a thin sheet of some stiff material (e.g., steel) with infinite extension. When specific control points along the plate are displaced, the plate undergoes deformation in such a way as to minimize the total bending energy E implied by the transformation.

The mathematical operations involved in the production of 2D thin-plate splines are described clearly by Trossman [19]. They can be extended to 3D.

Ferreira [20], a layerwise theory for composite and sandwich laminated plates discretized by the TPS method and concluded that the combination of adequate shear deformation theory and the TPS method allows a very accurate prediction of displacement and stresses.

Verpoest and Lomov [21] have achieved the modelling of fibre curves in fabric structure by bending energy in their geometric modelling studies of fabric structures. Similarly, they have modelled shape changes that occur under stretching, tension and pressure by bending energy.

When a woven fabric is subject to a ballistic impact, it undergoes deformation in vertical or perpendicular directions to the fabric plane. The deformation spreads out from the impact point within a certain speed interval. As speed increases since the energy of the bullet also increases, above a certain speed limit the bullet pierces and passes the fabric. During the ballistic impact, the spreading speed of the shock wave generated on the ballistic plane is related to the energy absorption capacity of plies and is important [22]. In systems with high wave spreading speed, more amount of energy can be damped. The energy on the fabric plies is damped by distribution and a certain portion of energy causes a trauma depression at the rear side of the material.

While the energy of the bullet spreads laterally, the unspread energy causes a trauma depth in the vertical direction. It is desired that energy is spread and damped, and this way the trauma depth is minimized. The events that occur in both directions are very complex and related to yarn qualities and weaving construction.

In the previous studies [23–32], ballistic performances of panels obtained from woven and unidirectional (UD) fabrics and/or their composites were investigated with different methods. While some of these studies [25–27] are related to the ballistic performance of soft fabrics, some have investigated the ballistic performance of composite panels [23, 24, 28–32]. The common point of all these studies is the investigation of the energy absorption capacity of fabrics and composites made of aramid and UHMWPE fibres used in ballistic protection [33]. The energy absorption and dissipation behaviour of fabrics and composites during ballistic impact and high-energy impact are quite complex. For this reason, during the impact, woven fabric's energy propagation behaviour along the fabric plane is important and should be examined. In the previous study [30], energy energy-propagating behaviour of panels made of Twaron fabrics was researched with the 2-D TPS method. At the end of the study, it was observed that the energy generates two separate effect zones on the fabric plane. The first effect zone is the region impact energy passes directly on the rear side of the fabric and the second zone is the area where the energy spreads on the fabric plane. The first zone is unwanted in terms of ballistic protection and the expansion of the dimensions of this zone indicates that a large portion of the energy passes behind. The second zone shows the propagating area of energy on the fabric plane.

Woven and unidirectional fabrics' energy propagating behaviour along the fabric plane during a ballistic impact is important and should be examined. In this study, impact energy's propagating behaviour along para-aramid woven and unidirectional fabric's plane will be researched with low-speed weight drop tests as in previous studies [30].

In addition, the effect of reinforcements in different directions on energy-propagating behaviour will be examined. For this purpose, plies of woven and unidirectional fabrics in different numbers will be tested in 0º/90º and 0º/90º/±45º yarn directions. The size of deformation that occurs after the ballistic impact will be determined and the fabric's energy-spreading behaviour on the plane will be found by using the shape changes due to deformation. To find energy propagating behaviours, the bending energy of fabrics will be calculated and energy propagating behaviours of woven and unidirectional structures will be compared in different yarn directions by determining expansion factors.

MATERIAL AND METHOD

Material

Ballistic fabrics

Twaron CT 710 type woven and K-Flex unidirectional nonwoven fabrics are used in this work. The properties of both fabrics are given in table 1.

K-Flex is not a woven fabric structure. K-Flex fabric is a nonwoven fabric which is formed by placing Kevlar 129 yarns at a right angle (at 0 and 90 degrees) on top of each other and then by sticking them with the help of pressure and temperature using polyethylene films (figure 1). No interlacing exists between the yarns perpendicular to each other and therefore K-Flex is a unidirectional nonwoven fabric structure. Because of this, no crimp is induced in the yarn [34]. Tests were carried out separately for woven and unidirectional fabrics. Both fabric types were converted into panels with 2, 4, 6 and 8 plies in 0º/90º directions and 2, 4 and 8 plies in 0º/90º/±45º directions. In preparation for 0º/90º/±45º panels, fabrics were cut diagonally at 45º to obtain ±45º fibre direction. Samples' distribution according to yarn direction is shown in table 2.

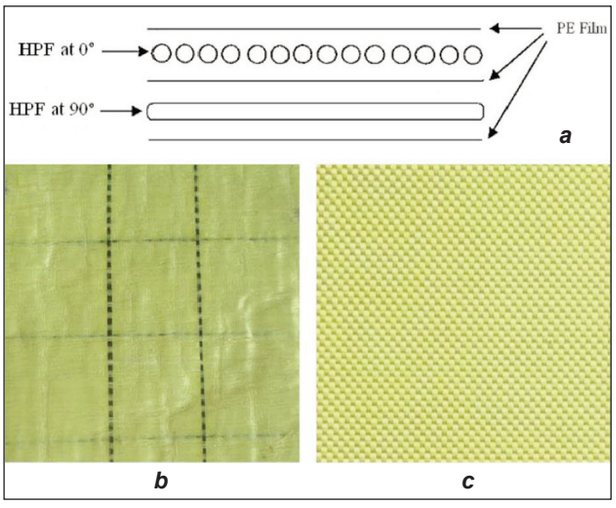

Fig. 1. Photos of: *a* – schematic representation of unidirectional non-woven fabric structure produced by placing yarns at a right angle on top of each other (at 0º and 90º) and then by sticking them using a polyethylene film (HPF: high-performance fibres); *b* – K-Flex UD woven fabric; *c* – Twaron CT 710 woven fabric

In samples prepared as 0º/90º/±45º, half of the plies were placed in normal directions, meaning 0º/90º, and the other half was placed in diagonal directions, meaning ±45º.

Test apparatus

The experiments we conducted in the ballistics laboratory were performed according to the drop test NIJ Standard-0101.06 [35] standard procedure, as seen in figure 2, *a* [9]. Various studies have been conducted in the literature using these standards [36–39]. The weights were released from a vertical distance of 1 meter and fell upon the clay surface. A pipe with a diameter of 50 mm was utilized to guide the weights.

Table 1

PROPERTİES OF TWARON CT 710 TYPE WOVEN AND K-FLEX UNİDİRECTİONAL NONWOVEN FABRİCS

Fabric type	Count (dtex) warp/weft (0°/90°)	Material type warp/weft	Weave	Density warp/weft (threads/10 cm)	Fabric weight (g/m^2)	Treatment	Thickness (mm)
Twaron CT 710	930/930	2040/2000	Plain	117/117	220	Scouring/ water-repellent treatment	0.3±0.1
K-Flex	935/935	Kevlar129/ Kevlar 129	Unidirectional (nonwoven)	100/100	185	-	0.2±0.1

Table 2

DISTRIBUTION OF SAMPLES USED IN TESTS ACCORDING TO YARN DIRECTIONS

Materials	Yarn orientation	1 ply	2 plies	4 plies	6 plies	8 plies
Twaron CT 710	0º/90º	+	+	+	+	+
	0º/90º/±45º		+	+		+
K-Flex	0º/90º	+	+	+	+	+
	0º/90º/±45º		+	+		+

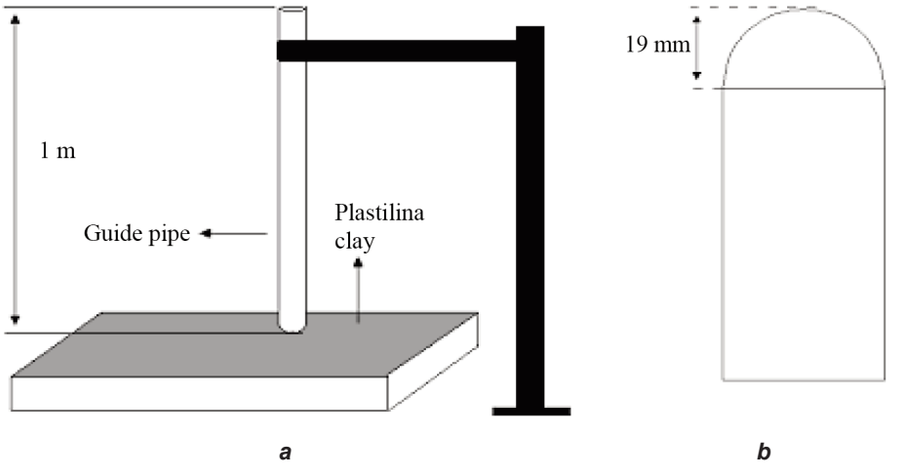

Fig. 2. Scheme of: *a* – test apparatus used in drop tests; *b* – weight used in drop tests [39, 40]

The weights have a 45 mm diameter, a hemispherical apex, and a 1 kg mass (figure 2, *b*).

The clay material employed in this research was No. 1 Type Roman Plastilina, which adheres to the NIJ criteria. The clay was placed in a box according to the given guidelines. The textiles were affixed by adhering tape to the front.

Figure 2 displays two-dimensional pictures. Drop tests are conducted on layers of fabric that are positioned on top of a clay foundation. The clay utilized is a specialized clay that is well-suited for the characteristics of human tissue. Based on the testing, it is determined that the deformation exhibited in clay is similar to the deformation that can occur in human tissue [40]. The calculation was carried out in four sequential steps. The initial stage entails the identification of landmarks from images, followed by the determination of their precise coordinates. The two numerals indicate the precise locations of the corresponding landmarks. These two forms can either represent individual samples or serve as a representation of the average of two sets of shapes that correspond to target landmarks. The process of transforming the source shape into the target shape requires moving the landmarks of the source to their corresponding landmarks in the target.

Method

The mechanism shown in figure 2 is used in the tests. Tests were performed by falling the weight from a 1-meter height. First, the weight was dropped on clay without using a cloth and the resulting shape deformation was photographed from a certain distance. Then, the weight was dropped on cloth layers consisting of 1, 2, 4, 6 and 8 layers respectively, and once more, the resulting shape deformation was photographed from a certain distance. Drop tests were applied on cloth layers on clay ground, and the deformation occurred on cloths after the tests were considered as deformation on clay. The computation proceeded in four steps. Firstly, landmarks are identified from photographs and then landmark coordinates are determined (figure 3).

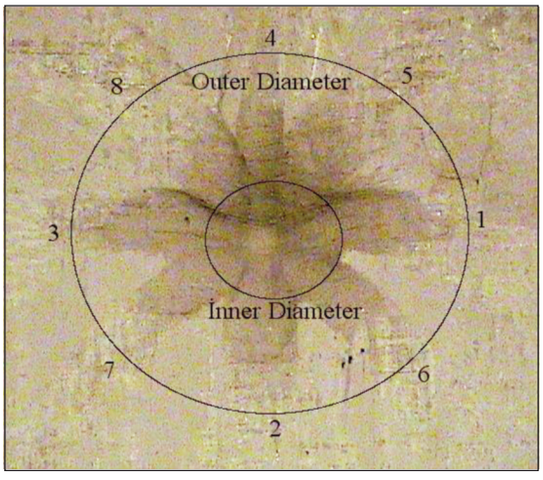

Fig. 3. İnner and outer diameter and landmarks from 1 to 8

Next, the mean landmark configurations are ascertained. In the last step, using average shapes obtained by Procrustes analysis, deformation shape (target) was practised using droppings of TPS rotating, round tip bullet on the empty ground with cloth layers (source). The bending energy causing the deformation was found by a program used in Matlab 7.0. Finally, expansion factors formed near the landmarks were calculated.

The coordinates of homologous landmarks from two shapes. These two shapes may represent either individual specimens or the means of two sets of shapes corresponding to target landmarks. A transformation from a source shape to a target shape involves the displacement of the source landmarks to the corresponding target landmarks [41].

We shall mainly concentrate on the important m = 2-dimensional case, with deformations given by the bivariate function

$$y = \phi(t) = \left(\phi_1(t), \phi_2(t)\right)^T \quad (1)$$

Bookstein [8] has developed a highly successful approach for deformations using a pair of thin-plate splines for the functions $\phi_1(t)$ ve $\phi_2(t)$. We concentrate on the important m = 2-dimensional case, the theory of which was developed by Duchon and Meinguet [42].

Consider the (2×1) landmarks t_j, j = 1,…,k, on the first figure mapped exactly into y_i, i = 1,…,k, on the second figure. We write $\phi(t_j) = (\phi_1(t_j), \phi_2(t_j))^T$, j = 1,…,k, for the two-dimensional deformation. Let,

$$T = [t_1 \;\; t_2 \;\; \ldots \;\; t_k]^T, \; Y = [y_1 \;\; y_2 \;\; \ldots \;\; y_k]^T$$

so that T and Y are both (k×2) matrices. A pair of thin-plate splines (PTPS) is given by the bivariate function

$$\phi(t) = (\phi_1(t), \phi_2(t))^T = c + At + W^T s(t) \qquad (2)$$

where t is (2×1), $s(t) = (\sigma(t - t_1), ..., \sigma(t - t_k))^T$, (k×1) and

$$\sigma(h) = \begin{cases} \|h\|^2 \log(\|h\|) & \|h\| > 0 \\ 0 & \|h\| = 0 \end{cases} \qquad (3)$$

The 2k+6 parameters of the mapping are c(2×1), A(2×2) and W(k×2). There are 2k interpolation constraints in Equation (1), and we introduce six more constraints for the bending energy in Equation (8) below to be defined.

$$1_k^T = 0, \;\; T^T W = 0 \qquad (4)$$

The pair of thin-plate splines which satisfy the constraints of Equation (4) are called natural thin_plate splines. Equations (1) ve (4) can be re-written in matrix form

$$\begin{bmatrix} S & 1_k & T \\ 1_k^T & 0 & 0 \\ T^T & 0 & 0 \end{bmatrix} \begin{bmatrix} W \\ c^T \\ A^T \end{bmatrix} = \begin{bmatrix} Y \\ 0 \\ 0 \end{bmatrix} \qquad (5)$$

where $(S)_{ij} = \sigma(t_i - t_j)$ and 1_k is the k-vector of ones. The matrix

$$\Gamma = \begin{bmatrix} S & 1_k & T \\ 1_k^T & 0 & 0 \\ T^T & 0 & 0 \end{bmatrix}$$

is symmetric positive definite and so the inverse exists, provided the inverse of S exists.

$$\begin{bmatrix} W \\ c^T \\ A^T \end{bmatrix} = \Gamma^{-1} \begin{bmatrix} Y \\ 0 \\ 0 \end{bmatrix}$$

Writing the partition of Γ^{-1} as

$$\Gamma^{-1} = \begin{bmatrix} \Gamma^{11} & \Gamma^{12} \\ \Gamma^{21} & \Gamma^{22} \end{bmatrix}$$

where Γ^{11} is k×k, it follows that

$$W = \Gamma^{11} Y$$
$$\begin{bmatrix} c^T \\ A^T \end{bmatrix} = [\hat{\beta}_1, \; \hat{\beta}_2] = \Gamma^{21} Y \qquad (6)$$

giving the parameter values for the mapping. If S^{-1} exists, then we have

$$\begin{aligned} \Gamma^{11} &= S^{-1} - S^{-1}Q(Q^T S^{-1} Q)^{-1} Q^T S^{-1}, \\ \Gamma^{12} &= (Q^T S^{-1} Q)^{-1} Q^T S^{-1} = (\Gamma^{21})^T, \\ \Gamma^{22} &= (Q^T S^{-1} Q)^{-1} \end{aligned} \qquad (7)$$

where $Q = [1_k, T]$. The k×k matrix B_e is called the bending energy matrix where

$$B_e = \Gamma^{11} \qquad (8)$$

There are constraints on the bending energy matrix

$$1_k^T B_e = 0, \quad T^T B_e = 0$$

and so the rank of the bending energy matrix is k–3. It can be proved that the transformation of Equation (5) minimizes the total bending energy of all possible interpolating functions mapping from T to Y, where the total bending energy is given by

$$J(\varphi) = \sum_{j=1}^{2} \iint_{R^2} \left(\frac{\partial^2 \varphi_j}{\partial x^2} \right)^2 + 2 \left(\frac{\partial^2 \varphi_j}{\partial x \partial y} \right)^2 + \left(\frac{\partial^2 \varphi_j}{\partial y^2} \right)^2 dx\, dy \qquad (9)$$

As a physical model, this idealization corporates several assumptions, such as zero energy cost for in-plane deformations [43].

A simple proof is given by Dryden and Mardia [41]. The minimized total bending energy is given by,

$$J(\varphi) = \text{trace}(W^T S W) = \text{trace}(Y^T \Gamma^{11} Y) \qquad (10)$$

Hence the minimum bending property of the TPS is highly suitable for many applications. The thin-plate spline has also proved popular because of the simple analytical solution [43].

Expansion factors are computed using the Jacobian of the warp [23]. For this purpose, weight was dropped first on the plain clay ground without fabrics and then on the fabric plies placed on the clay ground. The places of landmarks that belong to deformation caused by weight dropped on the plain ground change as a result of the drop tests done with fabric plies.

RESULTS AND DISCUSSION

Drop tests for woven and unidirectional fabrics and determination of deformation generated on the impact point along the fabric plane

Drop tests have been repeated 4 times for every sample and landmarks have been marked by photographing the deformation shape that occurred on the clay. Mean shapes have been constructed from the average values of the landmarks that express the shape.

It was observed that the deformation that occurred as a result of the drop tests done without fabric was virtually the same as the tip profile of the weight. Figure 4 shows the deformation that occurred as a result of the drop tests without fabric. Deformation shapes that occurred as a result of drop test done with plies of fabric; it was assumed that the deformation shape on the impact point is marked identically on the clay. Figure 5, *a* and *b* are the marks of deformation on the clay after drop tests with 0º/90º Twaron and 0º/90º K-Flex panels respectively. Examination

of these shapes indicates that deformation obtained from woven Twaron fabrics concentrates along weft and warp fibres. Twaron fabrics spread the energy more effectively in weft and warp fibre directions meaning 0º/90º however as seen in figure 5, *a* it can't spread well in diagonal directions. Therefore, the inner diameter that shows the impact effect is wider. Because K-Flex fabrics have no yarn curves in their structure, they can spread the impact energy more effectively along the fabric plane. As seen in figure 5, *b* the deformation on the impact point is circular and when compared Twaron panel, it is seen that deformation occurred in diagonal directions as well in addition to 0º/90º directions. This situation shows that K-Flex panels spread the energy to a wider area. Thus, the inner diameter that shows the impact effect is smaller. K-Flex's ability to spread energy to a larger area is due to a lack of bends between the yarns in its structure. This way, yarns can spread the energy better than woven structures in 0º and 90º directions.

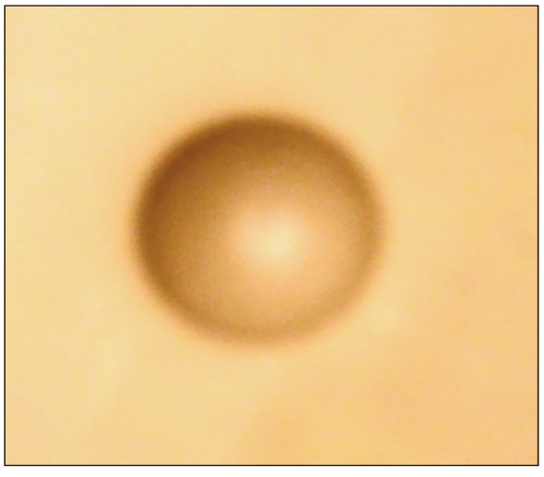

Fig. 4. The deformation shape caused by weight dropped on clay

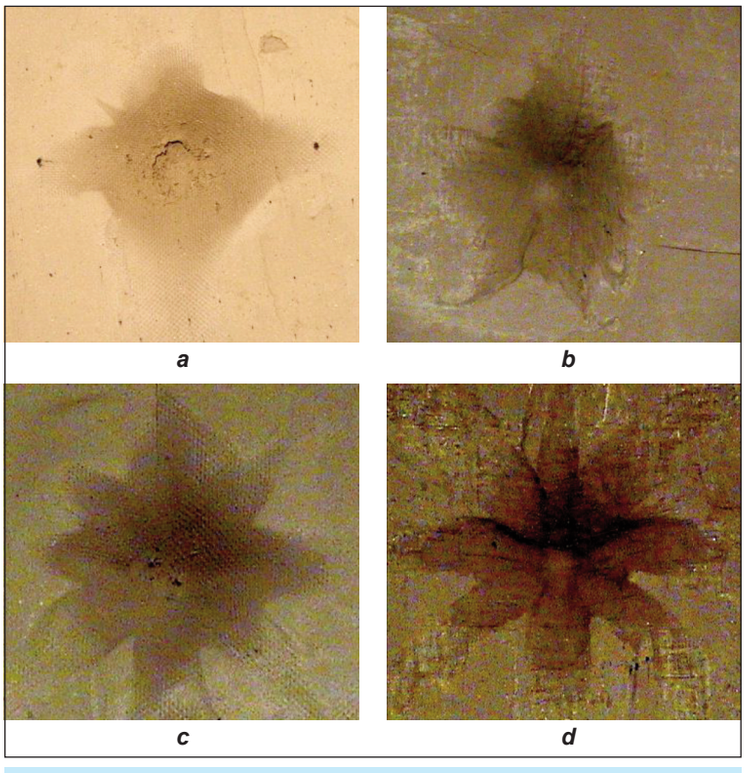

Fig. 5. The deformation shape caused by weight dropped on clay: *a* – 0º/90º Twaron panel; *b* – 0º/90º K-Flex panel; *c* – 0º/90º/±45º Twaron panel; *d* – 0º/90º/±45º K-Flex panel

Figure 5, *c* and d show respectively the shape of deformation in Twaron and K-Flex panels that have yarn reinforcements in 0º/90º/±45º directions. When they are compared to figure 5, *a* and *b*, deformation in a diagonal direction can be seen. This proves that yarn reinforcements in different directions increase the spreading area of the energy. In these structures, energy spreads not only in weft and warp fibre directions but also in ±45º diagonal directions. Thus, the measurement of the inner diameter caused by the impact effect decreases.

Figure 6 shows internal and external diameter measurements of deformation on the impact point. The diameter for 0º/90º-Twaron panels varies between 22.26 mm and 22.4 mm in 1 and 8 plies, and number of plies does not affect the inner diameter. Outer diameter for 0º/90º-Twaron panels varies between 32.63 mm and 39.94 mm in panels with 1 and 8 plies and as the number of plies increases the area of outer diameter also increases. In this case, we can say that as the number of fabric plies increases, energy's distribution area also increases. The inner diameter for 0º/90º/±45º-Twaron panels was 12.92 mm for 2 plies of fabric, and 9.62 mm for 8 plies of fabric. Similarly, the external diameter was 52.12 mm for 2 plies of fabric and 42.17 mm for 8-ply panels. In this case, both inner and outer diameters shrink; and it indicates that a significant amount of energy is damped and its impact on the rear side decreases. This means that yarn reinforcements in diagonal directions in panels made of woven fabrics help damping energy significantly. For 0º/90º-K-Flex panels, the inner diameter on the impact point varies between 20.4 and 21.12 between 1 and 8-ply panels. There is no significant difference between these values, and the inner diameter of K-Flex panels is between 9.7% and 5.7% smaller than Twaron panels. Similarly, outer diameter varies between 38.22 mm and 40.5 mm in 1 and 8-ply panels, and they are between 14.6% and 1.4% larger than Twaron panels. The larger outer diameter and smaller inner diameter in the deformation zone of K-Flex panels show that deformation generated by impact is spread to a larger area and the impact effect is not concentrated on a certain area. Inner diameter for 0º/90º/±45º-K-Flex panels was 13.3 mm in 2 ply panel, and 10.9 mm in 8 ply

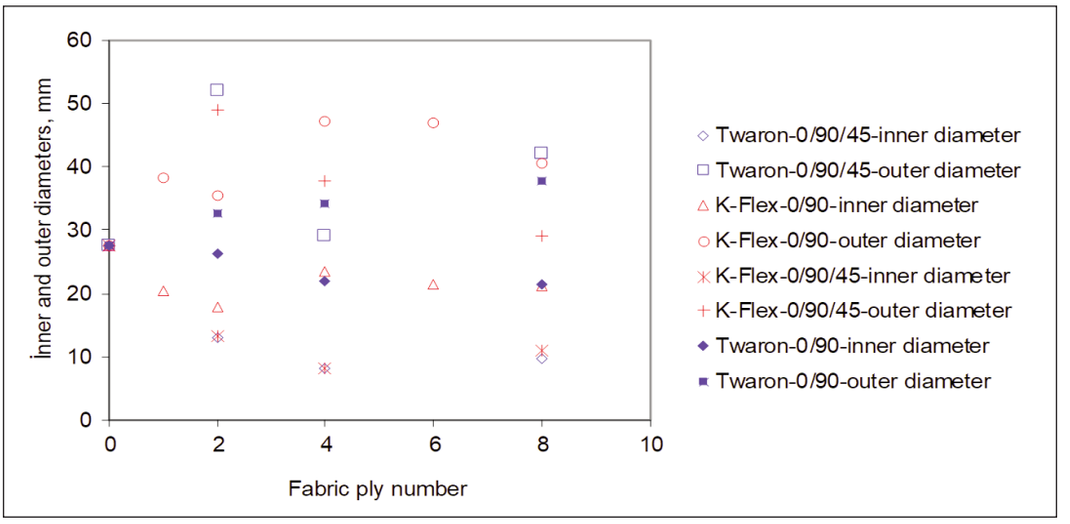

Fig. 6. Dimensions of deformation generated on impact point in woven and unidirectional panels about ply number (mm)

panel. Similarly, outer diameters were 49 mm in 2-ply panes and 29.02 mm in 8-ply panels. When these results are compared to those of Twaron panels, there are no significant differences between inner diameters however outer diameter measurements were 31.18% smaller in K-Flex panels.

When compared to panels with yarn reinforcements in 0º/90º directions, it was observed that the outer and inner diameters of panels with 0º/90º/±45º yarn reinforcements change significantly. In Twaron panels, the difference between 0º/90º and 0º/90º/±45º panels on average decreases by 55.39% in inner diameter measurements and increases by 49.34% in outer diameter measurements. This difference in K-Flex panels decreases by 70.60% in inner diameter and 7.5% in outer diameter. Thus, yarn reinforcements in diagonal directions support the spreading of deformation on the fabric plane and cause the fabric to absorb more energy. The decrease of both inner and outer diameters in K-Flex planes shows that energy is absorbed by the fabric before causing deformation and the dimensions of deformation shrink.

The ratios of outer and inner diameters to each other are given in table 3. According to this data, average outer/inner diameter ratios of Twaron and K-Flex panels that have 0º/90º yarn orientation are obtained as 1.61 and 1.99 respectively. Average outer/inner diameter ratios of Twaron and K-Flex panels that have 0º/90º/±45º yarn orientation are obtained as 3.99 and 3.64 respectively.

The determination of bending energy and expansion factors

The shape and dimensions of deformation generated along the fabric plane are determined above. In this section, the spreading behaviour of energy along the fabric plane has been determined by expansion factors. For this purpose, differences in shape deformations obtained after drop tests are analyzed by the TPS method. Bending energies are calculated by using equation number (10) with a program written under MATLAB 7.0 software. The results are given in table 4.

From table 4, it is seen that bending energy values don't change in relation to the number of fabric plies. In this case, average bending energies for Twaron and K-Flex panels with 0º/90º yarn directions are obtained as 2.94032 and 3.29037 respectively. Thus, the bending energy of K-Flex panels is 10.55% higher than Twaron panels. In Twaron and K-Flex panels with yarn reinforcements in 0º/90º/±45º directions, bending energy values are determined as 3.91739 and 4.03553 respectively. There is no significant difference between the bending energies of Twaron and K-Flex panels in this structure. When compared to

Table 3

OUTER DIAMETER/INNER DIAMETER RATIOS OF DEFORMATION GENERATED ON IMPACT POINT IN WOVEN AND UNIDIRECTIONAL PANELS IN RELATION TO PLY NUMBER

Materials	Yarn directions	Fabric ply number				
		1	2	4	6	8
Twaron CT710	0º/90º	1.24	1.55	1.76	1.75	1.78
	0º/90º/45º	-	4.03	3.58	-	4.38
K-Flex	0º/90º	1.87	1.99	2.02	2.19	1.92
	0º/90º/45º	-	3.68	4.58	-	2.66

Table 4

BENDING ENERGY VALUES ACCORDING TO THE NUMBER OF FABRIC PLIES AND YARN DIRECTIONS						
Materials	**Yarn directions**	**Fabric ply number**				
		1	**2**	**4**	**6**	**8**
Twaron CT710	0º/90º	2.9661	2.9361	2.9342	2.9326	2.9326
	0º/90º/45º	-	3.9151	3.91145	-	3.92563
K-Flex	0º/90º	3.21475	3.20357	3.25870	3.37663	3.39821
	0º/90º/45º	-	4.10284	4.80162	-	3.20215

panels with yarn reinforcements in 0º/90º directions, there are significant differences in bending energies of panels with 0º/90º/±45º fibre reinforcements. This difference is 24.8% in Twaron panels and 18.5% in K-Flex panels. Therefore, yarn reinforcements in diagonal directions have resulted in a very significant change in the bending energy.

Expansion factors which measure the expansions around selected landmarks are calculated according to the jakobien of warps. The locations of landmarks belonging to deformation generated by the weight dropped on the plain ground for this purpose change as a result of drop tests with fabric plies. These local expansions are given in tables 5–8. An example of this subject shows the shape deformation expansions after drop tests made with A-type weight on plain clay ground and 1 ply of K-Flex fabric in figure 7.

From table 5, it is seen that landmarks vary between 0.655 and 1.045. The most

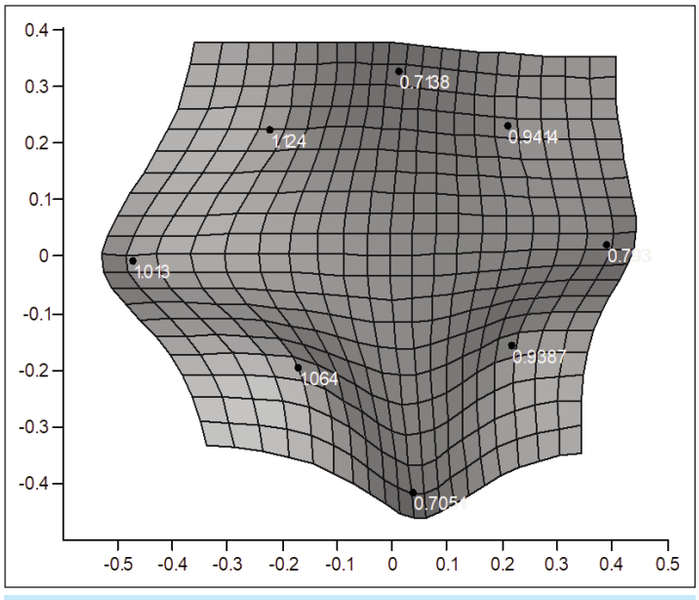

Fig. 7. The Expansion factors option will display the area expansions around each landmark indicating the degree of local growth

Table 5

EXPANSİON FACTORS FOR 0º/90º-TWARON FABRİCS AT THE LANDMARKS ARE SHOWN NUMERİCALLY								
Fabric ply number	**1. landmark**	**2. landmark**	**3. landmark**	**4. landmark**	**5. landmark**	**6. landmark**	**7. landmark**	**8. landmark**
1	0.984	0.944	0.987	1.045	0.687	0.712	0.695	0.702
2	0.975	0.988	0.996	1.012	0.715	0.720	0.789	0.655
4	1.030	0.994	0.966	1.005	0.785	0.673	0.858	0.921
6	1.008	0.987	0.987	0.988	0.877	0.686	0.775	0.954
8	1.008	0.987	0.988	1.012	0.866	0.721	0.668	0.753

Table 6

EXPANSİON FACTORS FOR 0º/90º-K-FLEX FABRİCS AT THE LANDMARKS ARE SHOWN NUMERİCALLY								
Fabric ply number	**1. landmark**	**2. landmark**	**3. landmark**	**4. landmark**	**5. landmark**	**6. landmark**	**7. landmark**	**8. landmark**
1	0.763	0.705	1.013	0.712	0.944	0.9387	1.064	1.124
2	0.8291	0.8997	0.9331	1.342	1.365	0.8461	1.146	1.094
4	0.7022	0.7281	0.8957	1.334	1.250	0.7051	0.5778	0.8265
6	1,1940	0.407	1.6064	1.139	0.4391	0.7831	0.8061	1.349
8	1.5100	0.8919	0.7894	0.475	0.6381	0.6439	1.111	1.087

Table 7

EXPANSİON FACTORS FOR 0º/90º/±45º-TWARON FABRİCS AT THE LANDMARKS ARE SHOWN NUMERİCALLY								
Fabric ply number	**1. landmark**	**2. landmark**	**3. landmark**	**4. landmark**	**5. landmark**	**6. landmark**	**7. landmark**	**8. landmark**
2	0.6217	1.0280	1.1410	1.1240	1.0590	1.0480	0.9262	0.5349
4	1.1920	1.1930	0.8923	0.8196	0.8424	1.1730	0.6830	0.6210
8	0.6971	0.8354	1.1170	0.9550	1.0590	0.9828	0.9597	0.7963

Table 8

EXPANSİON FACTORS FOR 0º/90º/±45º-K-FLEX FABRİCS AT THE LANDMARKS ARE SHOWN NUMERİCALLY								
Fabric ply number	**1. landmark**	**2. landmark**	**3. landmark**	**4. landmark**	**5. landmark**	**6. landmark**	**7. landmark**	**8. landmark**
2	0.5814	0.6935	0.8080	1.0880	0.5740	0.8696	1.2130	1.5120
4	0.8697	0.8422	1.3280	1.1970	0.7740	0.6535	0.7874	0.8120
8	1.0310	0.9420	0.8310	0.9060	1.1020	0.8934	0.8839	1.0450

remarkable result here is that expansion in landmarks number 1, 2, 3, 4 in 0º and 90º directions of Twaron panels with yarn reinforcements in 0º/90º directions are larger than landmarks number 5, 6, 7 and 8 in ±45º directions. This condition proves that expansion in diagonal directions is small and therefore deformation does not spread in these directions. When these results are compared to table 7, it is seen that expansions in landmarks number 1, 2, 3 and 4 in 0º and 90º directions are values close to landmarks number 5, 6, 7 and 8 and deviations in between are smaller. Therefore, we can say that yarn reinforcements in diagonal directions help the expansion and distribution of deformation on the fabric plane.

Tables 6 and 8 show expansion factors of K-Flex panels that have yarn reinforcements in 0º/90º and 0º/90º/±45º directions respectively. In table 6, there are no significant differences between expansions in landmarks number 5 6, 7 and 8 in ±45º directions and expansions in landmarks number 1, 2, 3 and 4 in 0º and 90º directions. This condition shows that even if there are no yarn reinforcements in the K-Flex panels' structure in diagonal directions, it can spread the deformation towards every direction along the fabric plane. Yarn reinforcements in diagonal directions will increase the capability of spreading the energy even further in these structures. In fact, it is seen in table 8 that expansion factors are higher compared to tables 5, 6 and 7 and both landmarks number 1, 2, 3 and 4 and landmarks number 5, 6, 7 and 8 have high values.

CONCLUSION

In this study, energy spreading behaviour of woven para-aramid fabric plies on impact point has been researched with drop tests and the following results have been found.

- The deformation area on the impact point is divided into two zones about energy fabric plies passing behind and energy fabric plies absorb by spreading on their plane. The energy fabric plies pass behind generates a deformation with a certain depth and diameter and this is the part with a small diameter and large depth (inner diameter). Deformation in this part has a circular form. The deformation generated in the area where energy is spread is distributed over a larger area and has a smaller depth (outer diameter).
- Dimensions of deformation generated by the energy that passes behind, meaning the measurements of inner and outer diameters vary according to the structure of fabric in used panels, the number of fabric plies and yarn reinforcement directions in panels.
- When 0º/90º-K-Flex panels are compared to Twaron panels, the inner diameter of K-Flex panels is between 9.7% and 5.7% smaller than Twaron panels. Similarly, the outer diameter is between 14.6% and 1.4% larger than Twaron panels. The larger outer diameter and a smaller inner diameter in the deformation zone of K-Flex panels show that deformation generated by impact is spread over a larger area and the impact effect is not concentrated on a certain area.
- When 0º/90º/±45º-K-Flex panels are compared to Twaron panels, there are no significant differences between inner diameters however the outer diameter in K-Flex panels is 31.18% smaller.
- In Twaron panels, while the difference between 0º/90º and 0º/90º/±45º panels on average decreases by 55.39% for inner diameter, outer diameter measurements have increased by 49.34%. In K-Flex panels, the same difference decreases by 70.60% for the inner diameter and 7.5% for the outer diameter.
- The diameter of the deformation generated by the energy that passes behind decreases in relation to the increase in the number of fabric plies. As the

number of fabric plies increases, the diameter of the area fabric plies distributes the energy also increases.

- The obtained expansion factor values show that Twaron woven fabric panels that have yarn reinforcements in 0º/90º directions distribute a significant portion of the energy along the weft and warp yarns. However unidirectional K-Flex panels with yarn reinforcements in 0º/90º directions can distribute the energy in more directions.
- Reinforcements in ±45° directions in addition to 0° and ±90° directions increased energy's spreading branches and therefore the diameter of the depression generated on the impact point, in other words, the amount of energy concentrating at one point has decreased.

REFERENCES

[1] Hanlon, E., Gillich, P., *Origin of the 44-mm behind-armor blunt trauma standard*, In: Mil. Med., 2012, 177, 333–339, https://doi.org/10.7205/MILMED-D-11-00303

[2] Gilson, L., Rabet, L., Imad, A., Kakogiannis, D., Coghe, F., *Development of a numerical model for the ballistic penetration of Fackler gelatine by small calibre projectiles*, In: Eur. Phys. J. Spec. Top., 2016, 2252, 225, 375–384, https://doi.org/10.1140/EPJST/E2016-02640-9

[3] Gilson, L., *Etude du comportement mécanique des multi-matériaux soumis à un impact balistique : approches expérimentale et numérique*, 2017

[4] Edwards, T.D., Bain, E.D., Cole, S.T., Freeney, R.M., Halls, V.A., Ivancik, J., Lenhart, J.L., Napadensky, E., Yu, J.H., Zheng, J.Q., Mrozek, R.A., *Mechanical properties of silicone based composites as a temperature insensitive ballistic backing material for quantifying back face deformation*, In: Forensic Sci. Int., 2018, 285, 1–12, https://doi.org/10.1016/J.FORSCIINT.2018.01.014

[5] Mukasey, M.B., Sedgwick, J.L., Hagy, D.W., *Ballistic Resistance of Personal Body Armor*, In: NIJ Standard-0101.06, NIJ Stand, 2008, 89

[6] Roberts, J.C., Ward, E.E., Merkle, A.C., O'Connor, J.V., *Assessing behind armor blunt trauma in accordance with the national institute of justice standard for personal body armor protection using finite element modeling*, In: J. Trauma – Inj. Infect. Crit. Care., 2007, 62, 1127–1133, https://doi.org/10.1097/01.TA.0000231779.99416.EE

[7] Mates, K.R.S.P., Forster, A., Riley, M., *Mechanical behaviour of ballistic clay as a function of temperature, pressure and strain rate*, In: Proc. Pers. Armour Syst. Symp., Cambridge, UK, 2014

[8] Hernandez, C., Buchely, M.F., Maranon, A., *Dynamic characterization of Roma Plastilina No. 1 from Drop Test and inverse analysis*, In: Int. J. Mech. Sci., 2015, 100, 158–168, https://doi.org/10.1016/J.IJMECSCI.2015.06.009

[9] Gilson, L., Rabet, L., Imad, A., Coghe, F., *Influence of plastilina properties and of repeated impacts during drop test*, In: Proc. 7th Symp. Light. Armour Gr. Def. Secur., 2019, 76–83

[10] Evci, C., Gülgeç, M., *Effective damage mechanisms and performance evaluation of ceramic composite armors subjected to impact loading*, In: J. Compos. Mater., 2014, 48, 3215–3236, https://doi.org/10.1177/0021998313508594

[11] Pereira, A.C., Lima, A.M., da C. Demosthenes, L.C., Oliveira, M.S., Costa, U.O., Bezerra, W.B.A., Monteiro, S.N., Rodriguez, R.J.S., Pinheiro, W.A., De Deus, J.F., *Ballistic Performance of Ramie Fabric Reinforcing*, In: Polymers (Basel), 2020, 12, 1–17

[12] Gilson, L., Rabet, L., Imad, A., Coghe, F., *Experimental and numerical assessment of non-penetrating impacts on a composite protection and ballistic gelatine*, In: Int. J. Impact Eng., 2020, 136, 103417, https://doi.org/10.1016/j.ijimpeng.2019.103417

[13] Alkhatib, F., Mahdi, E., Dean, A., *Design and evaluation of hybrid composite plates for ballistic protection: Experimental and numerical investigations*, In: Polymers (Basel), 2021, 13, 1–16, https://doi.org/10.3390/polym13091450

[14] Tan, V.B.C., Lim, C.T., Cheong, C.H., *Perforation of high-strength fabric by projectiles of different geometry*, In: Int. J. Impact Eng., 2003, 28, 207–222, https://doi.org/10.1016/S0734-743X(02)00055-6

[15] Carr, D.J., Horsfall, I., Malbon, C., *Is behind armour blunt trauma a real threat to users of body armour? A systematic review*, In: J. R. Army Med. Corps., 2016, 162, 8–11, https://doi.org/10.1136/JRAMC-2013-000161

[16] Ferreira, A.J.M., *Thin-Plate Splines for Thick Composite Plate Analysis*, In: Compos. Technol. 2020 Proc. Fourth Asian-Australasian Conf. Compos. Mater. (ACCM 4), 2004, 229–234, https://doi.org/10.1016/B978-1-85573-831-7.50044-4

[17] Bookstein, F.L., *Principal Warps: Thin-Plate Splines and the Decomposition of Deformations*, In: IEEE Trans. Pattern Anal. Mach. Intell., 1989, 11, 567–585, https://doi.org/10.1109/34.24792

[18] Bookstein, F.L., *Morphometric Tools for Landmark Data: Geometry and Biology, Morphometric Tools Landmark Data*, 1992, https://doi.org/10.1017/CBO9780511573064

[19] Trossman, D.S., Thompson, L.A., Hautala, S.L., *Application of thin-plate splines in two dimensions to oceanographic tracer data*, In: J. Atmos. Ocean. Technol., 2011, 28, 1522–1538, https://doi.org/10.1175/JTECH-D-10-05024.1

[20] Nguyễn, H., Fangueiro, R., Ferreira, F., Nguyễn, Q., *Auxetic materials and structures for potential defense applications: An overview and recent developments*, In: Text. Res. J., 2023, 93, 5268–5306

[21] Verpoest, I., Lomov, S.V., *Virtual textile composites software WiseTex: Integration with micro-mechanical, permeability and structural analysis*, In: Compos. Sci. Technol., 2005, 65, 2563–2574, https://doi.org/10.1016/J.COMPSCITECH.2005.05.031

[22] Zhu, X., Chen, W., L. Liu, K. Xu, G. Luo, Z. Zhao, *Experimental investigation on high-velocity impact damage and compression after impact behaviour of 2D and 3D textile composites*, In: Compos. Struct., 2023, 303, 116256, https://doi.org/10.1016/J.COMPSTRUCT.2022.116256

[23] Karahan, M., Karahan, E.A., *Development of an innovative sandwich composite material for protection of lower limb against landmine explosion: mechanical leg test results*, In: Text. Res. J., 2016, 87, 15–30, https://doi.org/10.1177/0040517515624880
[24] Karahan, M., Karahan, N., *Development of an innovative sandwich composites for the protection of lower limbs against landmine explosions*, In: J. Reinf. Plast. Compos., 2016, 35, 1776–1791, https://doi.org/10.1177/0731684416668261
[25] Karahan, M., Kuş, A., Eren, R., *An investigation into ballistic performance and energy absorption capabilities of woven aramid fabrics*, In: Int. J. Impact Eng., 2008, 35, 499–510, https://doi.org/10.1016/J.IJIMPENG.2007.04.003
[26] Karahan, M., Karahan, N., Nasir, M.A., Nawab, Y., *Effect of structural hybridization on ballistic performance of aramid fabrics*, In: J. Thermoplast. Compos. Mater., 2018, 32, 795–814, https://doi.org/10.1177/0892705718780197
[27] Karahan, M., *Comparison of Ballistic Performance and Energy Absorption Capabilities of Woven and Unidirectional Aramid Fabrics*, In: Text. Res. J., 2008, 78, 718–730, https://doi.org/10.1177/0040517508090487
[28] Karahan, M., Yildirim, K., *Low velocity impact behaviour of aramid and UHMWPE composites*, In: Fibres Text. East. Eur., 2015, 23, 97–105, https://doi.org/10.5604/12303666.1152522
[29] Khan, M.I., Umair, M., Hussain, R., Karahan, M., Nawab, Y., *Investigation of impact properties of para-aramid composites made with a thermoplastic-thermoset blend*, In: J. Thermoplast. Compos. Mater., 2021, 36, 866, https://doi.org/10.1177/08927057211021464
[30] Karahan, M., Jabbar, A., Karahan, N., *Ballistic impact behaviour of the aramid and ultra-high molecular weight polyethylene composites*, In: J. Reinf. Plast. Compos., 2015, 34, 37–48, https://doi.org/10.1177/0731684414562223
[31] Ari, A., Karahan, M., Kopar, M., Ahrari, M., *The effect of manufacturing parameters on various composite plates under ballistic impact*, In: Polym. Polym. Compos., 2022, 30, 1–15, https://doi.org/10.1177/09673911221144874
[32] Shaker, K., Jabbar, A., Karahan, M., Karahan, N., Nawab, Y., *Study of dynamic compressive behaviour of aramid and ultrahigh molecular weight polyethylene composites using Split Hopkinson Pressure Bar*, In: J. Compos. Mater., 2017, 51, 81–94, https://doi.org/10.1177/0021998316635241
[33] Joshi, A., Mishra, A., Saxena, V.K., *Impact response and energy absorption mechanisms of UHMWPE fabric and composites in ballistic applications: A comprehensive review*, In: Compos. Part A Appl. Sci. Manuf., 2024, 185, 108314, https://doi.org/10.1016/J.COMPOSITESA.2024.108314
[34] Gloger, M., Stempien, Z., Pinkos, J., *Numerical and experimental investigation of the ballistic performance of hybrid woven and embroidered-based soft armour under ballistic impact*, In: Compos. Struct., 2023, 322, 117420, https://doi.org/10.1016/J.COMPSTRUCT.2023.117420
[35] Mukasey, M.B., *Ballistic resistance of body armor NIJ standard-0101.06, Body Armor Ballist,* In: Stab Resist. Stand. with a Guid. to Sel., 2012, 1–62
[36] Gotts, P., *International ballistic and blast specifications and standards*, In: Light. Ballist. Compos. Mil. Law-Enforcement Appl. Second Ed., 2016, 115–156, https://doi.org/10.1016/B978-0-08-100406-7.00005-2
[37] Eaton, M.A.K., Henderson, K.A., McMahon, J.A., Salzar, R.S., *Testing the Validity of the NIJ Clay Standard for Approving Body Armor With a Preliminary Insight Into Injury Correlation*, In: ASME Int. Mech. Eng. Congr. Expo. Proc., 2021, 5, https://doi.org/10.1115/IMECE2020-23886
[38] Romano, T., Landheer, D., Williams, T., Bailey, S., Tomczyk, K., *Experimental-based numerical simulation of the drop test within NIJ Standard-0101.06 for personal hard armour development*, In: Pass, 2016
[39] Gilson, L., Rabet, L., Imad, A., Coghe, F., *Experimental and numerical characterisation of rheological properties of a drop test response of a ballistic plastilina*, In: Forensic Sci. Int., 2020, 310, 110238, https://doi.org/10.1016/J.FORSCIINT.2020.110238
[40] Abtew, M.A., Boussu, F., Bruniaux, P., Loghin, C., Cristian, I., *Engineering of 3D warp interlock p-aramid fabric structure and its energy absorption capabilities against ballistic impact for body armour applications*, In: Compos. Struct., 2019, 225, 111179, https://doi.org/10.1016/J.COMPSTRUCT.2019.111179
[41] Mardia, K.V., Dryden, I.L., *Shape distributions for landmark data*, In: Adv. Appl. Probab., 1989, 21, 742–755
[42] Dryden, I.L., Mardia, K.V., *General shape distributions in a plane*, In: Adv. Appl. Probab., 1991, 23, 259–276, https://doi.org/10.2307/1427747
[43] Hammer, O., *Paleontological Data Analysis*, 2007, 370, Available at: https://www.wiley.com/en-us/Paleontological+Data+Analysis-p-9781405172943 [Accessed on April 22, 2024]

Authors:

ALİ ARI[1], MEHMET KARAHAN[2,3]

[1]Department of Weapon Industry Technician, Vocational School of Higher Education, Ostim Technical University, 06374, Ankara, Türkiye

[2]Vocational School of Technical Sciences, Bursa Uludag University, 16059, Bursa, Türkiye
e-mail: mkarahan@uludag.edu.tr

[3]Butekom Inc., Demirtas Dumlupinar OSB District, 2nd Cigdem Street No:1/4, 16245, Osmangazi, Bursa, Türkiye

Corresponding author:

ALİ ARI
e-mail: ali.ari@ostimteknik.edu.tr